JACS
JOURNAL OF THE AMERICAN CHEMICAL SOCIETY
Article
pubs.acs.org/JACS

Measuring Selective Estrogen Receptor Modulator (SERM)–Membrane Interactions with Second Harmonic Generation

Grace Y. Stokes and John C. Conboy*

Department of Chemistry, University of Utah, 315 South 1400 East, Room 2020, Salt Lake City, Utah 84112, United States

Supporting Information

ABSTRACT: The interaction of selective estrogen receptor modulators (SERMs) with lipid membranes has been measured at clinically relevant serum concentrations using the label-free technique of second harmonic generation (SHG). The SERMs investigated in this study include raloxifene, tamoxifen, and the tamoxifen metabolites 4-hydroxytamoxifen, *N*-desmethyltamoxifen, and endoxifen. Equilibrium association constants (K_a) were measured for SERMs using varying lipid compositions to examine how lipid phase, packing density, and cholesterol content impact SERM-membrane interactions. Membrane-binding properties of tamoxifen and its metabolites were compared on the basis of hydroxyl group substitution and amine ionization to elucidate how the degree of drug ionization impacts membrane partitioning. SERM-membrane interactions were probed under multiple pH conditions, and drug adsorption was observed to vary with the concentration of soluble neutral species. The agreement between K_a values derived from SHG measurements of the interactions between SERMs and artificial cell membranes and independent observations of the SERMs efficacy from clinical studies suggests that quantifying membrane adsorption properties may be important for understanding SERM action in vivo.

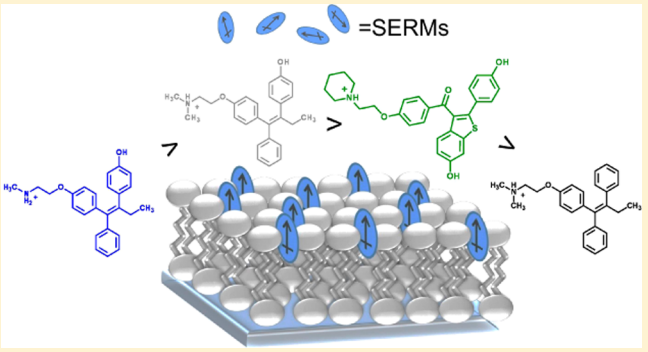

INTRODUCTION

Selective estrogen receptor modulators (SERMs) are a class of compounds that competitively bind to both nuclear and plasma membrane estrogen receptors to inhibit estrogen-induced breast tumor proliferation.[1−7] SERMs have also been shown to promote growth in bone, heart, and brain cells and are currently prescribed to prevent osteoporosis in postmenopausal women.[8−11] Tamoxifen (TAM) and raloxifene (RAL) are two FDA-approved SERMs that are widely prescribed to breast cancer patients and are recommended for use as preventative medications for women who are at increased risk for breast cancer.[12−15] At pH 7.4, the predominant forms of both TAM and RAL possess a +1 charge (Figure 1).[16,17] At this pH, TAM and RAL are expected to partition strongly into the plasma membrane based on their respective octanol–water distribution coefficients (log $D_{7.4}$) of 4.15 and 1.56.[16−18] However, these bulk phase distribution coefficients do not always adequately predict how drugs and cell membranes will interact,[19,20] mainly because the octanol–water interface does not account for the complexities of biological membranes.[21,22] Molecular-level interactions between drugs and natural cell membranes are difficult to monitor due to the diversity of lipids and proteins found in eukaryotic membranes.[23,24] Nonspecific interactions between SERMs and mammalian cell membranes can also control bioavailability and contribute to the drugs' anticancer actions but are poorly understood.[25−33]

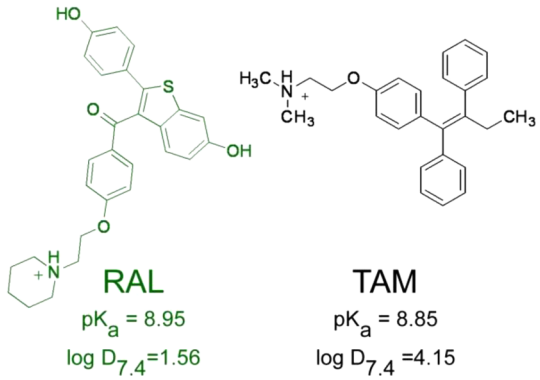

Figure 1. Chemical structures, pK_a values, and octanol–water distribution coefficients at pH 7.4 (log $D_{7.4}$) of RAL and TAM.

In vitro models can provide insight into drug–membrane interactions by providing a well-defined model. One easily prepared artificial membrane system that resembles a cell membrane in both thickness and fluidity is a planar supported lipid bilayer (PSLB).[34,35] In this work, PSLBs are used to measure the membrane binding properties of RAL, TAM, and three TAM metabolites. TAM metabolism is catalyzed by the cytochrome P450 enzymes, CYP 2D6 and CYP 3A4, to

Received: September 6, 2013
Published: January 10, 2014

   dx.doi.org/10.1021/ja409250y | J. Am. Chem. Soc. 2014, 136, 1409−1417

generate 4-hydroxytamoxifen (4-hydroxyTAM) and *N*-desmethyltamoxifen (*N*-desmethylTAM), respectively, which undergo secondary metabolism to endoxifen (Figure 2).[36,37] On a whole

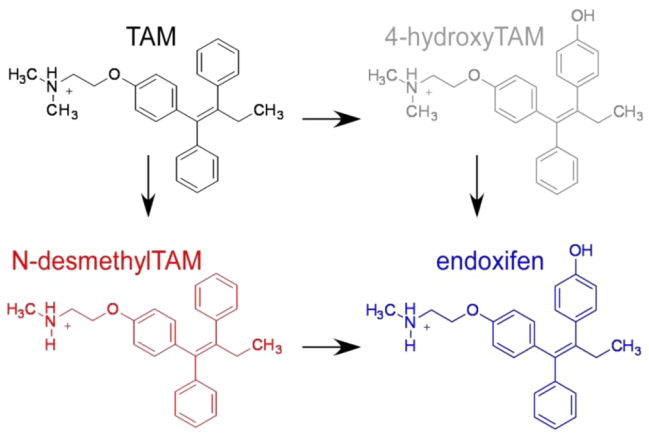

Figure 2. Chemical structures of the cytochrome P450 (CYP 2D6 and CYP 3A4) metabolites of TAM: 4-hydroxyTAM, *N*-desmethylTAM, and endoxifen.

cell or whole organism level, the clinical potency and antiestrogen effects of TAM metabolites differ widely from one another for reasons not fully understood.[36−40] Unlike TAM, RAL is not a prodrug because its glucuronide metabolites are less potent antiestrogens compared to the parent compound,[9,41] and membrane-binding properties of RAL metabolites are not addressed in this study.

Even though RAL gained FDA approval in September 2007, very few studies of the interactions between RAL and cell membranes have been published. Only one study was found that reported association constants, but this study monitored adsorption of RAL to sewage treatment solids.[16] Although membrane adsorption properties of RAL are not well studied, interactions between TAM and model membranes have been probed in a number of liposome systems using differential scanning calorimetry (DSC) and visible, infrared, and fluorescence spectroscopies.[26,27,29,30,42] However, the aforementioned studies used micromolar to millimolar total TAM concentrations, which are well above the concentrations found in the human body.[26−30,42,43] Blood plasma concentrations reported for TAM, 4-hydroxyTAM, *N*-desmethylTAM, and endoxifen are 300, 7, 700, and 180 nM, respectively.[38,39,44] Above 10 μM concentrations, TAM and its metabolites have been reported to exhibit detergent-like properties, causing lysis, deformation, cell-leakage, and solubilizing effects in membranes.[28] Likewise, at the micromolar concentrations that are generally used in laboratory studies, RAL forms insoluble colloids and oligomers.[16,45] These RAL complexes may behave differently than they do in the human body, where concentrations are reported to be 4 nM.[46−49] In order to access membrane adsorption at physiological concentrations, a highly sensitive, label-free analytical technique is needed.

The direct detection of low molecular weight small molecules associating to a membrane poses many challenges. Traditional methods for small molecule detection such as NMR or fluorescence require either isotopic labeling or the use of an exogenous fluorophore probe. Such modification, particularly the use of fluorescent markers, significantly alters the binding properties of the small molecule.[50−53] Other traditional analytical techniques such as differential scanning calorimetry, electrochemical methods, and surface plasmon resonance (SPR) lack the molecular specificity and detection limits required to observe biologically relevant concentrations of drug molecules.[54−56] One alternative method which has proven to be highly effective for quantifying interactions of small molecules with lipid membrane models in the label-free manner technique of second harmonic generation (SHG).[57]

In the study described below, SHG was used to quantify the adsorption of aqueous solutions of SERMs to PSLBs in a label-free manner and at biologically relevant concentrations. The work presented here provides a comprehensive comparison of the binding affinities of TAM, RAL, and the most active TAM metabolites, 4-hydroxyTAM and endoxifen, at concentrations ranging from 10 nM to 3 μM. In addition, the membrane composition of the PSLB was varied in order to investigate the effects of lipid phase, packing density, and cholesterol content on SERM-membrane interactions. The equilibrium association constants (K_a) that have been determined in this study can be used to predict drug−membrane interactions of similar drugs on the basis of the drug's chemical structure, pK_a values, and aqueous solubility.

SHG THEORY

SHG theory is described in detail elsewhere,[58] but here, we summarize briefly how SHG can be used to measure the adsorption of small molecules to lipid membranes. The SHG signal intensity (I_{SHG}) is resonantly enhanced when an adsorbed molecule exhibits an electronic transition near the incident (532 nm) or second harmonic (266 nm) wavelengths, as shown in the denominator of eq 1[59]

$$I_{SHG} \propto |\chi_R^{(2)}|^2 \propto \left| N \sum_{a,b,c} \frac{\langle a|\mu_i|c\rangle\langle a|\mu_j|b\rangle\langle b|\mu_k|c\rangle}{(2\hbar\omega - E_{ca} - i\Gamma_{ca})(\hbar\omega - E_{bc} - i\Gamma_{bc})} \right|^2 \quad (1)$$

Equation 1 describes SHG signal intensity (I_{SHG}) accounting only for contributions from the resonant term of the second-order susceptibility tensor squared ($|\chi_R^{(2)}|^2$), which varies with the surface density of adsorbed molecules squared (N^2). In eq 1, h is Plank's constant, ω is the frequency of incident light, Γ is the line width of the transition, μ is the dipole operator, and the subscripts a, b, and c are the initial, intermediate, and final states, respectively. In our experiments, I_{SHG} is measured as a function of bulk drug concentration [drug] to obtain an adsorption isotherm. The Langmuir model is used to fit these data and a nonlinear least-squares regression analysis is performed using the fitting parameters $(I_{SHG}^{max})^{1/2}$, the square root of the maximum SHG intensity at surface saturation, K_a, and [drug], as shown in eq 2

$$[\text{drug}]K_a = \frac{\sqrt{I_{SHG}}}{\sqrt{I_{SHG}^{max}} - \sqrt{I_{SHG}}} \quad (2)$$

The complete derivation of this expression has been published previously.[60] To obtain this simplified form of the Langmuir model, we assume that the nonresonant contribution to the SHG signal intensity is negligible compared to the resonant contribution, which is a valid approximation for our insulator quartz substrate in the presence of adsorbed SERM molecules.[61]

UV−vis spectra of the five SERM drugs investigated are shown in Figure 3. The second harmonic wavelength at 266 nm

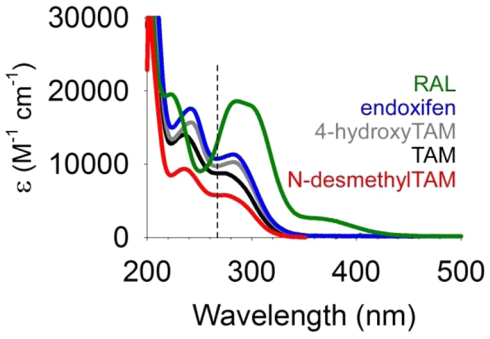

Figure 3. UV−vis spectra of all the SERMs investigated measured in PBS at pH 7.4. The dashed vertical line shows the second harmonic wavelength at 266 nm.

is noted with a dashed vertical line. For TAM and its metabolites, the extended conjugation of the triphenylethylene and for RAL, the conjugated π orbitals of the benzothiophene contribute to a strong electronic transition near 266 nm. The extinction coefficients at 266 nm (ε_{266nm}) measured in PBS at pH 7.4 for *N*-desmethylTAM, TAM, 4-hydroxyTAM, endoxifen, and RAL are 5800 ± 200, 8700 ± 400, 9700 ± 3000, 10700 ± 1000, and 12500 ± 1000 M^{-1} cm^{-1}, respectively. Because of these strong electronic resonances at 266 nm, the SHG response is resonantly enhanced as described in eq 1, providing a highly sensitive method for detecting SERM adsorption to a lipid bilayer.

EXPERIMENTAL SECTION

Materials. 1,2-dioleoyl-*sn*-glycero-3-phosphocholine (DOPC), 1,2-dimyristoyl-*sn*-glycero-3-phosphocholine (DMPC), 1,2-dipalmitoyl-*sn*-glycero-3-phosphocholine (DPPC), and 1,2-dioleoyl-*sn*-glycero-3-phospho-(1′-rac-glycerol) (DOPG) were purchased from Avanti Polar Lipids. Lipid stock solutions in chloroform (25 mg/mL) were used as received. Cholesterol (CHO) was purchased from Sigma Aldrich (Sigma grade, ≥99%) and was dissolved in spectroscopy grade chloroform (Omnisolv) to 10 mg/mL. All SERMs used, including tamoxifen (≥99%), raloxifene hydrochloride (>99%), (*E*/*Z*)-endoxifen hydrochloride hydrate (≥99%), (*Z*)-4-hydroxytamoxifen (≥99%), and *N*-desmethyltamoxifen HCl (≥98%), were purchased from Sigma-Aldrich and used without further purification. The SERMs were first dissolved in methanol (HPLC grade, Fisher) to prepare stock solutions, which were stored at 4 °C and used within three months. Phosphate buffered saline (PBS buffer) containing 50 mM sodium phosphate (Mallinckrodt) and 100 mM sodium chloride (Macron) was adjusted to pH 7.4 with sodium hydroxide (Mallinckrodt), unless otherwise specified. Solution pH was measured using an Accumet pH combination electrode (Fisher Scientific) connected to an Orion 720A meter. For the pH-dependent studies, all PBS solutions contained 50 mM sodium phosphate, but the total ionic strength was maintained at 0.15 M by varying the sodium chloride concentration. Binding isotherms were obtained using a range of bulk SERM concentrations—from 10 nM to 3 μM. These solutions were prepared daily by diluting stock SERM solutions in methanol with PBS buffer. The resulting solutions had a total methanol concentration (v/v) of less than 0.1%. All aqueous SERM solutions were purged with nitrogen for at least 30 min before use in the SHG binding experiments.

Lipid Bilayer Preparation. Silica prisms and Teflon flow cells were cleaned in a 70:30 v:v solution of 18 M sulfuric acid (Fisher Scientific) and 30% hydrogen peroxide (ACS grade, Fisher Scientific) for a minimum of 4 h. (*CAUTION: This solution is a strong oxidant and reacts violently with organic solvents. Extreme caution must be taken when handling this solution*). Immediately before lipid bilayer deposition, the substrate and Teflon flow cell were washed with copious amounts of NANOpure Infinity Ultrapure water (Barnstead/Thermolyn) with a minimum resistivity >18 MΩ cm. Fused silica prisms were cleaned with Ar plasma (Harrick Scientific Plasma Cleaner/Sterilizer) for 3 min before being mounted to the Teflon flow cell.

PSLBs were formed on the fused silica prism substrates (full spectrum grade IR-UV, Almaz Optics) by incubating the surface with small unilamellar vesicles (SUVs).[62] The SUVs were prepared by combining the appropriate volumes of stock lipid and CHO solutions followed by vortexing. The lipid mixture solutions (1 mg/mL) were evaporated under a gentle stream of N_2(g) and vacuum-dried overnight to remove residual chloroform. Dried lipid mixtures were stored at −20 °C. Dried lipids were resuspended in PBS buffer (1 mg/mL) followed by vortexing and bath sonication for at least 20 min or until solutions were clear. Saturated lipids required heating above the phase transition temperature (T_m). Two milliliters of the SUV solution were injected into a custom-built Teflon flow cell (volume ∼0.4 mL) and incubated with the prism substrate for 20 min. A minimum of 10 mL of PBS buffer was flushed through the flow cell to remove any unbound lipids.

Counter-Propagating SHG Setup. Our counter-propagating SHG setup has been described in detail elsewhere.[58,63] Briefly, a Q-switched Nd:YAG laser (Continuum) with a 7 ns pulse width at a repetition rate of 10 Hz was used to generate a collimated beam (3 mm in diameter). The energy of this 532 nm visible light source was attenuated to 10 mJ/pulse and directed onto a fused silica prism at an incident angle of 67° under total internal reflection. The reflected beam was steered back onto the prism surface using a 0° 532 nm/1064 nm dielectric mirror (ThorLabs) and spatially overlapped with the incident beam to generate second harmonic light (2ω = 266 nm), which was emitted along the surface normal. The SHG was measured using a photomultiplier tube (Hamamatsu R7154) and processed with a gated integrator (Stanford Research Systems). PSLBs were incubated at room temperature with each SERM solution for at least 30 min (and up to 5 h for lowest concentrations) and the SHG signal was recorded. To ensure that the drug concentration in the bulk phase above the PSLB was not depleted by adsorption, at least 6 injections of the same concentration of each SERM were introduced into the flow cell until a steady-state SHG response was obtained. Day-to-day laser fluctuations were accounted for by a two point normalization procedure using the SHG signal intensities recorded from a 10 mM potassium hydroxide solution and a PBS buffer solution at pH 7.4.

RESULTS

The binding isotherms of RAL, TAM, and the three cytochrome P450 metabolites of TAM adsorbed to DOPC, DMPC, DOPC+30 mol % CHO are shown in Figure 4. As discussed in the SHG Theory section above, the Langmuir model was fit to the isotherm data shown in Figure 4 to obtain the equilibrium binding constants. Table 1 summarizes the K_a values of each SERM adsorbed to DOPC, DMPC, and DOPC +30 mol % CHO. K_a values were found to increase in the following order: TAM < RAL < *N*-desmethylTAM < 4-hydroxyTAM < endoxifen. Because *N*-desmethylTAM exhibited a low membrane affinity to DOPC, which was not

Table 1. Binding Constants (K_a) for SERMs Interacting with DOPC, DMPC, and DOPC + 30% CHO

	DOPC K_a (× 10^6 M^{-1})	DMPC K_a (× 10^6 M^{-1})	DOPC+30% CHO K_a (× 10^6 M^{-1})
RAL	2.4 ± 0.2	1.2 ± 0.2	2.5 ± 0.1
TAM	2.0 ± 0.1	1.2 ± 0.2	1.7 ± 0.2
endoxifen	11.3 ± 0.8	9.1 ± 0.7	5.3 ± 0.3
4-hydroxyTAM	8.8 ± 0.6	2.6 ± 0.7	5.8 ± 0.6
N-desmethylTAM	2.9 ± 0.4		

dx.doi.org/10.1021/ja409250y | *J. Am. Chem. Soc.* 2014, 136, 1409−1417

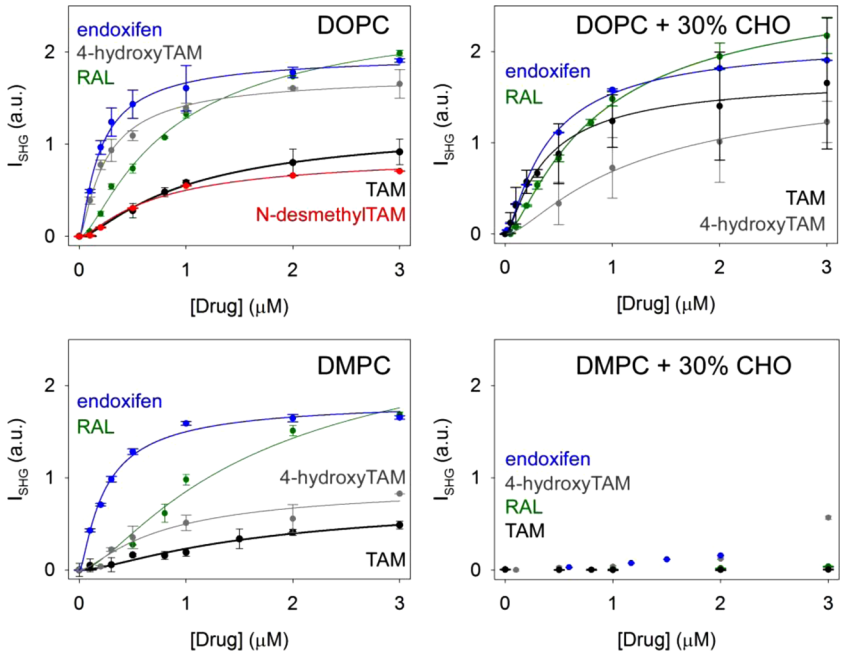

Figure 4. SHG signal intensities as a function of bulk endoxifen, 4-hydroxyTAM, RAL, TAM, and *N*-desmethylTAM concentration. Isotherms describe drug adsorption to PSLBs composed of DOPC (top left), DMPC (bottom left), DOPC + 30% CHO (top right), and DMPC with 30% CHO (bottom right). Solid lines represent fits to the data using the Langmuir model, eq 2.

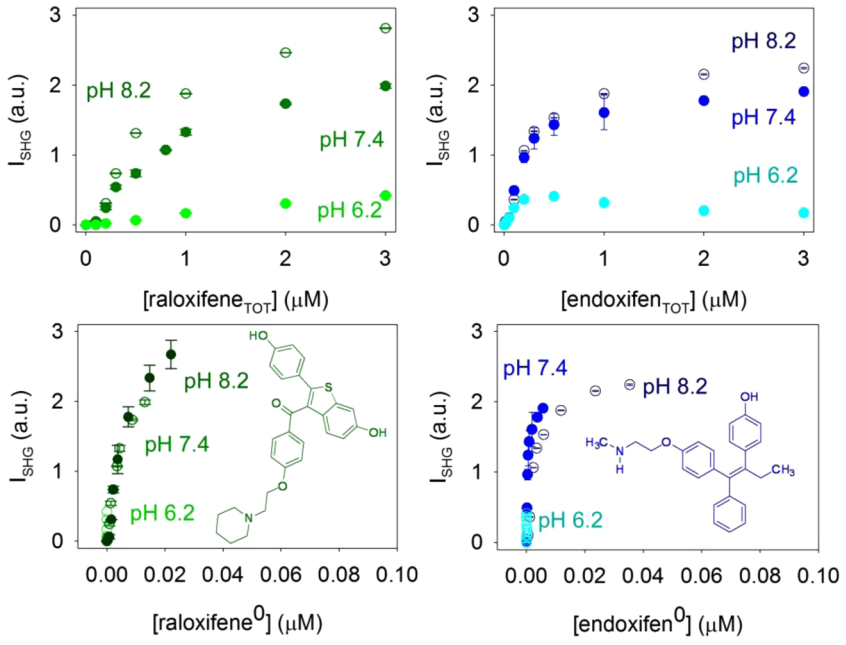

Figure 5. SHG signal intensity measured for the adsorption of raloxifene (left) and endoxifen (right) to a DOPC membrane at pH 6.2, 7.4, and 8.2 as a function of concentration of total (top) and neutral (bottom) forms of the drug species.

significantly different from the binding constants measured for TAM, its adsorption to DMPC, DOPC+30 mol % CHO, DMPC+30 mol % CHO, and DPPC was not investigated. The isotherm data from the adsorption of the SERMs to DMPC+30 mol % CHO were not fit to the Langmuir equation as no specific binding was observed. I_{SHG}^{max} values obtained from the Langmuir fits are 0.9 ± 0.1, 1.7 ± 0.2, 1.8 ± 0.1, 2.0 ± 0.1, and 2.6 ± 0.1 for *N*-desmethylTAM, TAM, 4-hydroxyTAM, endoxifen, and RAL adsorbed to DOPC, respectively.

To address the issue that I_{SHG} depends not only on the number of drug molecules adsorbed to the PSLB but is also correlated with the orientation and order of the drug molecules in the lipid bilayer, we conducted polarization-resolved SHG measurements to probe whether the orientation of TAM adsorbed in a DOPC lipid bilayer are the same at both low and high surface densities.[64,65] The results of these polarization-resolved SHG experiments suggest that the orientation of the SERM molecules intercalated into the lipid bilayer does not change with increasing surface densities, as discussed in detail in the Supporting Information.

It has been suggested in previous studies that the neutral form of the SERM is responsible for membrane binding.[66] To

dx.doi.org/10.1021/ja409250y | J. Am. Chem. Soc. 2014, 136, 1409−1417

better understand the impact of ionization state on SERM adsorption, we monitored endoxifen and RAL (the two SERMs that exhibited the highest SHG signal intensities) adsorption to PSLBs of DOPC at a pH of 6.2, 7.4, and 8.2, the results of which are summarized in Figure 5. We predicted that binding affinities should vary with the concentrations of neutral SERM species. To test this hypothesis, the SHG signal intensities were plotted as a function of the concentration of the neutral form of RAL and endoxifen. Based on the published pK_a values of RAL and endoxifen,[16,67] we calculated the relative concentrations of the ionized and neutral SERM species at pH 6.2, 7.4, and 8.2, which are listed in Table 2 (see Supporting Information for calculations). In addition, differences in solubilities between RAL and endoxifen as a function of pH were also accounted for in the data presented in Figure 5. Solubility calculations are detailed in the Supporting Information.

Table 2. pK_a Values for TAM, 4-HydroxyTAM, RAL, and Endoxifen Used To Calculate the Percentages of Cationic and Neutral SERM Species at pH 6.2, 7.4, and 8.2

		cationic:neutral		
	pK_a	pH 6.2	pH 7.4	pH 8.2
TAM	8.85	99.8:0.2	96.5:3.5	81.5:18.5
4-hydroxyTAM	8.86	99.8:0.2	96.6:3.4	81.9:18.1
RAL	8.95	99.8:0.2	97.2:2.8	84.7:15.3
endoxifen	10.13	99.99:0.01	99.8:0.2	98.8:1.2

The SHG data obtained from our adsorption isotherm experiments cannot directly be used to quantify the SERM surface density (Γ). In the linear region of the binding isotherms, at low surface densities, we expect no competition for binding sites.[5] Thus, the partitioning of the drug in the membrane can be equated to the drug concentration in the membrane of solution phase liposomes. The membrane partition coefficients ($P_{membrane}$) of tamoxifen (TAM) and 4-hydroxytamoxifen (4-hydroxyTAM) in liquid crystalline (l.c.) phase DMPC liposomes at 37 °C were reported by Custódio et al. to be 3×10^3 M^{-1} and 3.3×10^4 M^{-1}, respectively.[6] The 10-fold difference in $P_{membrane}$ was attributed to the phenolic substituent. Seydel suggested that the polar hydroxyl group may increase H-bonding between the drug molecule and the phospholipid head groups at the surface of the bilayer, which in turn disrupts the membrane, decreases lipid packing density, and allows more space for the drug to intercalate.[7] The $P_{membrane}$ values reported by Custódio et al.[6] were used to calculate Γ for TAM and 4-hydroxyTAM using eq 3

$$[\mathrm{SERM}]_{membrane} = P_{membrane}[\mathrm{SERM}]_{bulk} \quad (3)$$

The membrane concentration ($[\mathrm{SERM}]_{membrane}$) in molecules/cm^2 was determined by assuming that the DOPC bilayer has an effective thickness of 50 Å. In order to calibrate the measured SHG intensity with the surface density of the drugs, a sensitivity factor (*sensitivity*) was calculated by correlating the SHG signal intensity with surface excess (Γ) at low bulk SERM concentrations. In Figure 6, Γ was plotted as a function of bulk SERM concentration. The calculated saturation concentration, or maximum surface excess (Γ_{max}), was determined by fitting the data in Figure 6 to the Langmuir equation.

For 4-hydroxyTAM, $\Gamma_{max} = 3.06 \pm 0.05 \times 10^{10}$ molecules/cm^2 and for TAM, $\Gamma_{max} = 1.6 \pm 0.1 \times 10^{10}$ molecules/cm^2. On the basis of the calculated *sensitivity*, we determined the limit of detection (LOD) for TAM and 4-hydroxyTAM using eq 4,

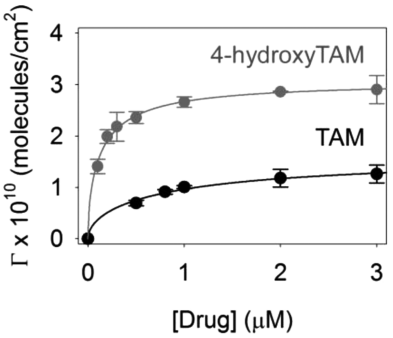

Figure 6. Surface excess (Γ) for 4-hydroxyTAM and TAM. Solid lines are fits to the data using the Langmuir model.

where σ is the standard deviation of the SHG signal for a blank (no drug present)

$$\mathrm{LOD} = \frac{3\sigma}{sensitivity} \quad (4)$$

The LOD values for TAM and 4-hydroxyTAM were determined to be 0.09 ± 0.02 and 0.13 ± 0.02 pg/cm^2, respectively, and are reported in Table 3. In the cases of RAL, endoxifen, and *N*-desmethylTAM, membrane partition coefficients have not been determined experimentally. Therefore, calculations of the $[\mathrm{SERM}]_{membrane}$ for these drugs required estimating $P_{membrane}$ from bulk octanol–water partition coefficients (P_{OW}). This procedure is described in the Supporting Information.

Table 3. Membrane Partition Coefficients (log $P_{membrane}$) Reported by Custódio et al.,[43] Used To Calibrate Adsorption Isotherm Data To Determine the Maximum Surface Excess (Γ_{max}) and Limit of Detection for TAM and 4-HydroxyTAM

	log $P_{membrane}$	$\Gamma_{max} \times 10^{10}$ (molecules/cm^2)	LOD (pg/cm^2)
TAM	3.5	1.6 ± 0.1	0.09 ± 0.02
4-hydroxyTAM	4.5	3.06 ± 0.05	0.13 ± 0.04

DISCUSSION

Impact of Lipid Phase and Packing Density on SERM Adsorption. All SERMs investigated adsorbed to a DOPC (T_m = −20 °C, in the l.c. phase at 23 °C) lipid bilayer with higher K_a values as compared to those of a DMPC (T_m= 23 °C, coexistence of the l.c. and gel phases at 23 °C) lipid bilayer. For example, the K_a value calculated for 4-hydroxyTAM adsorbed to DOPC is 8.8 ± 0.6 × 10^6 M^{-1}, whereas the K_a value calculated for 4-hydroxyTAM adsorbed to DMPC is 2.6 ± 0.7 × 10^6 M^{-1}, a decrease of 70%. Likewise, the K_a values for RAL, TAM, and endoxifen adsorbed to DOPC are 50%, 45%, and 19% higher, respectively, than RAL, TAM, and endoxifen adsorbed to DMPC. The K_a of RAL adsorbed to DMPC in a mixed gel and l.c. phase coexistence at room temperature was the same, within error, as the K_a of RAL adsorbed to gel phase DMPC at 10 °C (see Supporting Information). Therefore, further investigations of SERM adsorption to gel phase DMPC were not conducted. At the concentrations under investigation, SERMs did not adsorb to lipid bilayers composed of DPPC (T_m = 41 °C, in the gel phase at 23 °C), as shown in the Supporting Information. The differences in binding affinities between DOPC, DMPC, and DPPC are attributed to

dx.doi.org/10.1021/ja409250y | J. Am. Chem. Soc. 2014, 136, 1409–1417

differences in packing densities. In our studies, all five SERMs adsorbed to DMPC lipids at room temperature with lower binding constants compared to l.c. phase DOPC lipids. The mean molecular area (MMA) of DMPC at 22 °C was measured to be 58 Å^2 at a surface pressure (Π) of 30 mN/m.[68,69] In contrast, the limiting area per molecule of DOPC lipids at the collapse pressure (46 mN/m) was 67.5 Å^2.[70] Thus, significantly more space between lipids is available for drug intercalation in DOPC bilayers compared to DMPC bilayers, which may account for differences in binding constants. The MMA of DPPC lipids is about 50 Å^2,[70] which suggests that SERMs do not adsorb to DPPC because the closely packed acyl chains did not allow for small molecule penetration. The loose packing of the acyl chains of DOPC and DMPC allowed sufficient space for SERMs to intercalate.

Role of CHO on SERM Binding. CHO is important to cell function and is a major component of plasma membranes.[24,71] The presence of CHO alters the physical structure of a cell membrane[71−76] and, therefore, may change how drug molecules adsorb. Generally, CHO exhibits a condensing effect on lipid bilayers because the lipid acyl chains become more tightly packed upon CHO intercalation.[72] Relevant concentrations of CHO in mammalian cell membranes range from 0 to 30 mol %.[71] Drug association was monitored in DOPC, DMPC, and DPPC lipid bilayers containing 30 mol % CHO. Although this CHO concentration is on the high end of the biologically relevant concentration spectrum, it was chosen because 30 mol % CHO places DOPC and DMPC lipid membranes in the liquid ordered phase,[72,77] which is predicted to change the adsorption properties of the SERMs.

The impact of CHO on SERM binding was monitored, and the resulting adsorption isotherms are shown in the top right and bottom right graphs of Figure 4. In the presence and absence of 30 mol % CHO, K_a values of RAL binding to DOPC are statistically identical. However, the K_a values calculated for TAM binding to DOPC + 30 mol % CHO decrease slightly to $1.7 \pm 0.2 \times 10^6$ M^{-1}. The largest changes in K_a values due to the presence of 30 mol % CHO were observed for endoxifen and 4-hydroxyTAM, where decreases of 53% and 34% to $5.3 \pm 0.3 \times 10^6$ M^{-1} and $5.8 \pm 0.6 \times 10^6$ M^{-1}, respectively, were observed. A greater change in the phase state of the membrane is caused by addition of CHO to DMPC compared to DOPC.[76] Addition of 30 mol % CHO inhibits adsorption of all four SERMs to DMPC lipid bilayers, as shown in the bottom right graph in Figure 4. The presence of 30 mol % CHO may cause the DMPC lipid acyl chains to pack more densely, preventing penetration of SERMs. These results are consistent with previous studies that indicate that adding 30 mol % CHO to DMPC lipids shifts the lipid phase from the liquid-disordered to the liquid-ordered phase, where inadequate space was available between the tightly packed DMPC acyl chains for bulky SERM molecules to intercalate.[72] Our work agrees with results published by Custódio et al., who also observed that in the presence of 20 mol % CHO, TAM did not incorporate into DMPC liposomes.[43] Our results also agree with observations reported previously in our lab for two other small molecules, tetracaine[57,79] and merocyanine (MC540).[78] For example, both in the absence and in the presence of 28 mol % CHO, binding constants for tetracaine to DOPC were statistically identical.[57] However, in the presence of 28 mol % CHO incorporated in a DMPC lipid bilayer at 27 °C, tetracaine exhibited a 41% lower K_a value than in the absence of CHO.[57] Likewise, MC540 adsorption to DOPC lipids did not change in the presence of 33 mol % CHO, but for DMPC lipids, fluorescence signal intensities were 50% lower in the presence of CHO.[78]

Membrane Adsorption Properties of TAM Metabolites. TAM and its three metabolites allow us to methodically quantify the relative impact on membrane adsorption of two structural variants, the (1) substitution of a hydroxyl group and (2) degree of amine substitution. Both the amine and hydroxyl functional groups are expected to impact drug binding to lipid bilayers.[66,80,81] However, the relative impact of each functional group on membrane adsorption is not well understood.[82,83] In place of a hydrogen atom in the para position of the triphenylethylene ring in TAM and *N*-desmethylTAM, a phenolic hydroxyl group is present in 4-hydroxyTAM and endoxifen. As shown in Table 1, the K_a value of endoxifen adsorbed to DOPC is nearly four times higher than the K_a value calculated for *N*-desmethylTAM, which lacks a hydroxyl substituent. Likewise, the K_a value of 4-hydroxyTAM adsorbed to DOPC is six times higher than the K_a value calculated for TAM. Because of the presence of a hydroxyl group, these more polar metabolites may interact more strongly with the zwitterionic phosphocholine head groups, which may result in the higher K_a values observed. Our work agrees with the results published by Wiseman et al., who studied the effects of 0 to 45 μM TAM, *N*-desmethylTAM, and 4-hydroxyTAM premixed in ox-brain phospholipid liposomes.[29] Wiseman et al. observed that 4-hydroxyTAM caused a significant decrease in lipid fluidity, whereas the ordering effects of TAM and *N*-desmethylTAM were smaller in magnitude.[29] Our work is also in agreement with results published by Custódio et al., who observed a higher membrane affinity for 4-hydroxyTAM compared to TAM.[43] The higher membrane affinity was attributed to interactions between the hydroxyl group in 4-hydroxyTAM and the zwitterionic phosphocholine headgroup of DMPC. Custódio et al. argued that adsorption of 4-hydroxyTAM perturbed hydrogen bonding and destabilized the lipid bilayer, allowing higher concentrations of the drug to partition into the DMPC membrane.[43]

The influence of hydroxyl-substitution in the membrane association of other small molecules has been investigated by a number of researchers. Wesolowska et al. studied resveratrol and its hydroxyl-substituted metabolite piceatannol interactions with model membranes composed of DPPC and DMPC using DSC and electron paramagnetic resonance (EPR).[84] The results reported by Wesolowska et al. are consistent with our observations that the hydroxyl-substituted analogues adsorb more strongly to lipid bilayers than the parent compound.[84] Likewise, Van Dael and Ceuterickx compared the effects of membrane partitioning between phenol and benzene and suggested that phenol adsorbed near the polar headgroup, whereas benzene partitions into the hydrophobic portion of the lipid bilayer.[85] Our results combined with previously published drug-membrane studies suggest that the substitution of a hydroxyl group strongly influences a drug's binding affinity and may control the location in the PSLB where a SERM adsorbs. In addition to the presence of a hydroxyl functional group, the presence of an amine substituent may also influence the binding properties of SERMs.

TAM and 4-hydroxyTAM are tertiary amines, whereas *N*-desmethylTAM and endoxifen are secondary amines. At pH 7.4, as shown in Table 2, 3.5% of the total 4-hydroxyTAM in solution is predicted to be in the neutral form. In comparison, only 0.2% of the total endoxifen in solution is in the neutral form. A similar difference in % neutral species is expected for

tertiary amine tamoxifen versus secondary amine *N*-desmethyltamoxifen. The neutral form of a drug is thought to adsorb to the cell membrane.[86] However, TAM and 4-hydroxyTAM do not exhibit higher K_a values than *N*-desmethylTAM and endoxifen, respectively. As shown in Table 1, at pH 7.4, the K_a value calculated for endoxifen adsorbed to DOPC is 28% higher than the K_a value for 4-hydroxyTAM adsorbed to DOPC, and the K_a value for *N*-desmethylTAM adsorbed to DOPC is 45% higher than the K_a value for TAM adsorbed to DOPC. One reason that the K_a values do not scale with the concentrations of neutral SERM species, ($[SERM^0]$) is because in aqueous solution, the solubility of the secondary amines, endoxifen, and *N*-desmethylTAM is five times higher than the solubility of the tertiary amines, 4-hydroxyTAM, and TAM, because of hydrogen bonding interactions.[87]

Effect of $[SERM^0]$ and Solubility on SERM Adsorption. SHG intensities measured for endoxifen and RAL adsorbed to DOPC as a function of total and neutral SERM species concentrations, $[SERM_{TOT}]$ and $[SERM^0]$, respectively, at pH 6.2, 7.4, and 8.2 are shown in Figure 5. Adsorption to DOPC as a function of $[SERM_{TOT}]$ increases with increasing pH. This trend is not surprising as $[SERM^0]$ increases with pH and the neutral form of each SERM is expected to adsorb more strongly to DOPC than its cationic form. As shown in Table 2, $[RAL^0]$ is 0.2%, 2.8%, and 15.3% of $[RAL_{TOT}]$, whereas $[endoxifen^0]$ is 0.01%, 0.2% and 1.2% of $[endoxifen_{TOT}]$ at pH 6.2, 7.4, and 8.2, respectively. SHG signal intensities are plotted as a function of $[RAL^0]$ and $[endoxifen^0]$ in the bottom left and right graphs, respectively, of Figure 5. The adsorption isotherms for endoxifen binding to DOPC at pH 6.2 and pH 7.4 overlap with the isotherm data at pH 8.2. At pH 8.2, endoxifen is more than 20 times more soluble than RAL.[16,88−92] Although neutral endoxifen species are expected to be fully soluble at the concentrations used in our experiments, only 5% of the neutral RAL species is soluble and available to adsorb to DOPC at pH 8.2. When solubility differences are accounted for, the binding isotherms of $[RAL^0]$ to DOPC at pH 6.2, 7.4, and 8.2 overlap, indicating that membrane interactions vary with the concentration of dissolved neutral species. The results of these pH studies suggest that SERM adsorption depends not only on the $[SERM^0]$ but also on the solubility of neutral SERM species.

Maximum Surface Excess and LOD for TAM and 4-HydroxyTAM. The maximum surface excess (Γ_{max}) of TAM and 4-hydroxyTAM adsorbed to DOPC lipid membranes at room temperature were calculated and are reported in Table 3. The nearly 2-fold higher Γ_{max} of 4-hydroxyTAM compared to TAM may be attributed to the 10-fold higher membrane partition coefficient of 4-hydroxyTAM compared to TAM. The sensitivity factors used to calculate Γ_{max} were also used to determine the limits of detection (LOD) of TAM and 4-hydroxyTAM. LOD values are also reported in Table 3. These LOD values are between one and 3 orders of magnitude lower than LOD values obtained by UV−SFG spectroscopy for azithromycin (3.6 ± 0.3 pg/cm^2) and tolnaftate (1306.8 ± 52.8 pg/cm^2) adsorbed to DOPC lipid bilayers.[8]

Membrane Adsorption Properties of SERMs Correlate with In Vivo Studies. The results presented in Figure 4 and Table 1 show that RAL and TAM adsorb to DOPC and DMPC lipid bilayers with similar K_a values even though bulk-phase log $D_{7.4}$ values shown in Figure 1 differ by 2 orders of magnitude.[16] However, our results correlate well with clinical studies that indicate that RAL and TAM exhibit similar efficacy in breast cancer treatments and similar effects on heart, bone, and brain health.[8] The K_a values calculated from our binding isotherms also coincide with the results of in vivo studies of TAM metabolites, which indicate that TAM and *N*-desmethylTAM are less effective antiestrogens compared to endoxifen and 4-hydroxyTAM.[38,82,93,94] Our results also suggest that endoxifen is a highly membrane-active SERM and may exhibit a high affinity for estrogen receptors located in the plasma membrane,[5,33,95,96] as it also exhibits a strong affinity for nuclear estrogen receptors.[32] In February 2013, phase 1 clinical trials were underway at the National Cancer Institute to test endoxifen's use as a breast cancer drug.[38−40,93,94,97] The membrane association constants measured in vitro can help clinicians better understand endoxifen's activity and potency in vivo. Specific interactions between SERMs and estrogen receptor targets strongly influence the drug's clinical efficacy. However, in order for the drug to interact with an estrogen receptor, it must first interact with the lipids in the cell membrane. Our studies suggest that quantifying the nonspecific interactions between SERMs and lipid membranes provides the foundation needed to further investigate the interactions between these drugs and membrane-bound estrogen receptors.

■ SUMMARY

Counter-propagating SHG was used to monitor the interactions between SERMs and PSLBs at clinically relevant drug concentrations without extrinsic labels. K_a values measured for SERMs adsorbed to the l.c. phase lipids, DOPC, were higher than K_a values measured for SERMs adsorbed to DMPC, which is in a mixed gel and l.c. phase coexistence. SERMs did not adsorb to gel phase DPPC lipids. These results were attributed to space constraints in the tightly packed gel-phase lipids, which did not allow small molecules to penetrate. The presence of 30 mol % CHO did not inhibit adsorption of SERMs to DOPC. However, 30 mol % CHO significantly lowered the binding affinities of SERMs to DMPC, which was attributed to the condensing effects of CHO in DMPC lipids. Binding isotherms measured at pH 6.2, 7.4, and 8.2 overlapped if both the solubilities and concentrations of neutral SERM species were taken into account. In our investigations, K_a values measured for the hydroxyl-substituted metabolites of TAM, 4-hydroxyTAM and endoxifen, were three times higher than binding constants measured for TAM or *N*-desmethylTAM, which lacked a hydroxyl group. In clinical studies, hydroxyl-substituted TAM metabolites exhibited the highest activities and drug efficacies compared to TAM or *N*-desmethylTAM. Our studies provide a compelling argument for a strong correlation between a drug's activity and its membrane affinity, which is most likely related to the fact that some of the estrogen receptors that SERMs target are membrane-bound proteins. Ongoing investigations of the interactions between SERMs and membrane-bound estrogen receptors are being conducted in our laboratory.

■ ASSOCIATED CONTENT

Ⓢ Supporting Information

Polarization-resolved SHG signal intensities for TAM adsorbed to DOPC monitored in a copropagating geometry at low and high surface densities. Adsorption isotherms of RAL adsorbed to DMPC in the gel phase, RAL and TAM adsorbed to anionic lipids, and RAL, TAM and endoxifen adsorbed to DPPC and DPPC with 30 mol % CHO. Calculations of the ratios of neutral and anionic SERM species, RAL solubility, fluorescence images to confirm stability of PSLBs in the presence of high

RAL concentrations, kinetic analysis of endoxifen binding, and calculation of maximum surface excess and limits of detection of RAL, endoxifen, and *N*-desmethylTAM. This material is available free of charge via the Internet at http://pubs.acs.org

AUTHOR INFORMATION

Corresponding Author

conboy@chem.utah.edu

Notes

The authors declare no competing financial interest.

ACKNOWLEDGMENTS

The authors acknowledge the financial support from the National Institutes of Health (R01-GM068120). Any opinions, findings, conclusions, or recommendations expressed in this material are those of the authors and do not necessarily reflect the views of the National Institutes of Health.

REFERENCES

(1) Shang, Y.; Brown, M. *Science* **2002**, *295*, 2465−2468.
(2) Brzozowski, A. M.; Pike, A. C. W.; Dauter, Z.; Hubbard, R. E.; Bonn, T.; Engstrom, O.; Ohman, L.; Greene, G. L.; Gustafsson, J.-A.; Carlquist, M. *Nature* **1997**, *389*, 753−758.
(3) Levin, E. R. *Mol. Endocrinol.* **2005**, *19*, 1951−1959.
(4) Prossnitz, E. R.; Arterburn, J. B.; Smith, H. O.; Oprea, T. I.; Sklar, L. A.; Hathaway, H. J. *Annu. Rev. Physiol.* **2008**, *70*, 165−190.
(5) Levin, E. R. *Mol. Endocrinol.* **2011**, *25*, 377−384.
(6) Revankar, C. M.; Cimino, D. F.; Sklar, L. A.; Arterburn, J. B.; Prossnitz, E. R. *Science* **2005**, *307*, 1625−1630.
(7) Govind, A. P.; Thampan, R. V. *Mol. Cell. Biochem.* **2003**, *253*, 233−240.
(8) Barrett-Connor, E.; Mosca, L.; Collins, P.; Geiger, M. J.; Grady, D.; Kornitzer, M.; McNabb, M. A.; Wenger, N. K. *N. Engl. J. Med.* **2006**, *355*, 125−137.
(9) Dodge, J. A.; Lugar, C. W.; Cho, S.; Short, L. L.; Sato, M.; Yang, N. N.; Spangle, L. A.; Martin, M. J.; Phillips, D. L.; Glasebrook, A. L.; Osborne, J. J.; Frolik, C. A.; Bryant, H. U. *J. Steroid Biochem. Mol. Biol.* **1997**, *61*, 97−106.
(10) Dutertre, M.; Smith, C. L. *J. Pharmacol. Exp. Ther.* **2000**, *295*, 431−437.
(11) Morello, K. C.; Wurz, G. T.; DeGregorio, M. W. *Clinical Pharmacokinetics* **2003**, *42*, 361−372.
(12) Dowers, T. S.; Qin, Z.-H.; Thatcher, G. R. J.; Bolton, J. L. *Chem. Res. Toxicol.* **2006**, *19*, 1125−1137.
(13) Lewis, J. S.; Jordan, V. C. *Mutat. Res., Fundam. Mol. Mech. Mutagen.* **2005**, *591*, 247−263.
(14) Michael, H.; Harkonen, P. L.; Kangas, L.; Vaananen, H. K.; Hentunen, T. A. *Br. J. Pharmacol.* **2007**, *151*, 384−395.
(15) Nelson, H. D.; Smith, M. E. B.; Griffin, J. C.; Fu, R. *Ann. Intern. Med.* **2013**, *158*, 604−614.
(16) Teeter, J. S.; Meyerhoff, R. D. *Environ. Toxicol. Chem.* **2002**, *21*, 729−736.
(17) Avdeef, A. *Adsorption and drug development: solubility, permeability, and charge state*; John Wiley & Sons: Hoboken, NJ, 2003.
(18) Scherrer, R. A.; Howard, S. M. *J. Med. Chem.* **1977**, *20*, 53−58.
(19) Mason, R. P.; Chester, D. W. *Biophys. J.* **1989**, *56*, 1193−1201.
(20) Hallifax, D.; Houston, J. B. *Drug Metab. Dispos.* **2007**, *35*, 1325−1332.
(21) Leahy, D. E.; Morris, J. J.; Taylor, P. J.; Wait, A. R. *J. Chem. Soc., Perkin Trans.* **1992**, *2*, 705−722.
(22) Leahy, D. E.; Morris, J. J.; Taylor, P. J.; Wait, A. R. *J. Chem. Soc., Perkin Trans.* **1992**, *2*, 723−731.
(23) Lingwood, D.; Simons, K. *Science* **2010**, *327*, 46−50.
(24) van Meer, G.; Voelker, D. R.; Feigenson, G. W. *Nat. Rev. Mol. Cell. Biol.* **2008**, *9*, 112−124.
(25) Clarke, R.; van den Berg, H. W.; Murphy, R. F. *J. Natl. Cancer Inst.* **1990**, *82*, 1702−1705.
(26) Custódio, J. A.; Almeida, L. M.; Madeira, V. M. C. *Biochim. Biophys. Acta* **1993**, No. 1150, 123−129.
(27) Dicko, A.; Morissette, M.; Ben Ameur, S.; Pézolet, M.; Di Paolo, T. *Brain Res. Bull.* **1999**, *49*, 401−405.
(28) Engelke, M.; Bojarski, P.; Bloß, R.; Diehl, H. *Biophys. Chem.* **2001**, *90*, 157−173.
(29) Wiseman, H.; Quinn, P.; Halliwell, B. *FEBS Lett.* **1993**, *330*, 53−56.
(30) Kazanci, N.; Severcan, F. *Biosci. Rep.* **2007**, *27*, 247−255.
(31) Duval, D.; Durant, S.; Homo-Delarche, F. *Biochim. Biophys. Acta* **1983**, *737*, 409−442.
(32) Thomas, P.; Dong, J. *J. Steroid Biochem. Mol. Biol.* **2006**, *102*, 175−179.
(33) Levin, E. R. *Trends Endocrin. Met.* **2009**, *20*, 477−482.
(34) Castellana, E. T.; Cremer, P. S. *Surf. Sci. Rep.* **2006**, *61*, 429−444.
(35) Plant, A. L. *Langmuir* **1999**, *15*, 5128−5135.
(36) Dickschen, K.; Willmann, S.; Thelen, K.; Lippert, J.; Hempel, G.; Eissing, T. *Front. Pharmacol.* **2012**, *3*, 1−15.
(37) Jordan, V. C. *Nat. Rev. Drug. Discov.* **2003**, *2*, 205−213.
(38) Hawse, J. R.; Subramaniam, M.; Cicek, M.; Wu, X.; Gingery, A.; Grygo, S. B.; Sun, Z.; Pitel, K. S.; Lingle, W. L.; Goetz, M. P.; Ingle, J. N.; Spelsberg, T. C. *PLoS One* **2013**, *8*, e54613.
(39) Lim, Y. C.; Li, L.; Desta, Z.; Zhao, Q.; Rae, J. M.; Flockhart, D. A.; Skaar, T. C. *J. Pharmacol. Exp. Ther.* **2006**, *318*, 503−512.
(40) Johnson, M. D.; Zuo, H.; Lee, K.-H.; Trebley, J. P.; Rae, J. M.; Weatherman, R. V.; Desta, Z.; Flockhart, D. A.; Skaar, T. C. *Breast Cancer Res. Treat.* **2004**, *85*, 151−159.
(41) Kemp, D. C.; Fan, P. W.; Stevens, J. C. *Drug Metab. Dispos.* **2002**, *30*, 694−700.
(42) Bilge, D.; Kazanci, N.; Severcan, F. *J. Mol. Struct.* **2013**, *1040*, 75−82.
(43) Custódio, J. A.; Almeida, L. M.; Madeira, V. M. C. *Biochem. Biophys. Res. Commun.* **1991**, No. 176, 1079−1085.
(44) Aranda, E. O.; Esteve-Romero, J.; Rambla-Alegre, M.; Peris-Vicente, J.; Bose, D. *Talanta* **2011**, *84*, 314−318.
(45) Doak, A. K.; Wille, H.; Prusiner, S. B.; Shoichet, B. K. *J. Med. Chem.* **2010**, *53*, 4259−4265.
(46) Jagadish, B.; Yelchuri, R.; K, B.; Tangi, H.; Maroju, S.; Rao, V. U. *Chem. Pharm. Bull.* **2010**, *58*, 293−300.
(47) Baer, B. R.; Wienkers, L. C.; Rock, D. A. *Chem. Res. Toxicol.* **2007**, *20*, 954−964.
(48) Jeong, E. J.; Lin, H.; Hu, M. *J. Pharmacol. Exp. Ther.* **2004**, *310*, 376−385.
(49) Trontelj, J.; Vovk, T.; Bogataj, M.; Mrhar, A. *Pharmacol. Res.* **2005**, *52*, 334−339.
(50) Barghouthi, S.; Eftink, M. R. *Biophys. Chem.* **1993**, *46*, 13−19.
(51) Zhang, J.; Hadlock, T.; Gent, A.; Strichartz, G. R. *Biophys. J.* **2007**, *92*, 3988−4001.
(52) Auger, M.; Jarrell, H. C.; Smith, I. C. P. *Biochemistry* **1988**, *27*, 4660−4667.
(53) Boulanger, Y.; Schreier, S.; Smith, I. C. P. *Biochemistry* **1981**, *20*, 6824−6830.
(54) Campos, R.; Kataky, R. *J. Phys. Chem. B* **2012**, *116*, 3909−3917.
(55) Ducey, M. W., Jr; Smith, A. M.; Guo, X.; Meyerhoff, M. E. *Anal. Chim. Acta* **1997**, *357*, 5−12.
(56) Zhou, B.; Zhang, Z.; Zhang, Y.; Li, R.; Xiao, Q.; Liu, Y.; Li, Z. *J. Pharm. Sci.* **2009**, *98*, 105−113.
(57) Nguyen, T. T.; Conboy, J. C. *Anal. Chem.* **2011**, *83*, 5979−5988.
(58) Conboy, J. C.; Kriech, M. A. *Anal. Chim. Acta* **2003**, *496*, 143−153.
(59) Shen, Y. R. *The Principles of Nonlinear Optics*; Wiley: New York, 1984.
(60) Nguyen, T. T.; Sly, K. L.; Conboy, J. C. *Anal. Chem.* **2011**, *84*, 201−208.
(61) Corn, R. M.; Higgins, D. A. *Chem. Rev.* **1994**, *94*, 107−125.
(62) Kalb, E.; Frey, S.; Tamm, L. K. *Biochim. Biophys. Acta* **1992**, *1103*, 307−316.

(63) Kriech, M. A.; Conboy, J. C. *J. Opt. Soc. Am. B* **2004**, *21*, 1013−1021.
(64) Shen, Y. R. *Annu. Rev. Phys. Chem.* **1989**, *40*, 327−350.
(65) Zhang, T. G.; Zhang, C. H.; Wong, G. K. *J. Opt. Soc. Am. B* **1990**, *7*, 902−907.
(66) Smith, D. A.; van de Waterbeemd, H.; Walker, D. K. Absorption. In *Pharmacokinetics and Metabolism in Drug Design*; Wiley-VCH Verlag GmbH & Co. KGaA: Weinheim, 2006; pp 39−53.
(67) Law, B. *J. Chromatogr. A* **1987**, *407*, 1−18.
(68) Gudmand, M.; Fidorra, M.; Bjørnholm, T.; Heimburg, T. *Biophys. J.* **2009**, *96*, 4598−4609.
(69) Castelli, F.; Sarpietro, M. G.; Rocco, F.; Ceruti, M.; Cattel, L. *J. Colloid Interface Sci.* **2007**, *313*, 363−368.
(70) Andrade, C. A. S.; Baszkin, A.; Santos-Magalhães, N. S.; Coelho, L. C. B. B.; de Melo, C. P. *J. Colloid Interface Sci.* **2005**, *289*, 379−385.
(71) Yeagle, P. L. *Biochim. Biophys. Acta* **1985**, *822*, 267−287.
(72) Almeida, P. F. F.; Vaz, W. L. C.; Thompson, T. E. *Biochemistry* **1992**, *31*, 6739−6747.
(73) de Meyer, F.; Smit, B. *Proc. Natl. Acad. Sci. U. S. A.* **2009**, *106*, 3654−3658.
(74) Finegold, L. *Cholesterol in membrane models*; CRC Press: Boca Raton, 1993.
(75) Martinez-Seara, H.; Róg, T.; Pasenkiewicz-Gierula, M.; Vattulainen, I.; Karttunen, M.; Reigada, R. *Biophys. J.* **2008**, *95*, 3295−3305.
(76) Róg, T.; Pasenkiewicz-Gierula, M.; Vattulainen, I.; Karttunen, M. *Biochim. Biophys. Acta* **2009**, *1788*, 97−121.
(77) Polozov, I. V.; Gawrisch, K. *Biophys. J.* **2006**, *90*, 2051−2061.
(78) Smith, K. A.; Conboy, J. C. *Biochim. Biophys. Acta* **2011**, *1808*, 1611−1617.
(79) Nguyen, T. T.; Rembert, K.; Conboy, J. C. *J. Am. Chem. Soc.* **2011**, *133*, 6096−6097.
(80) Seddon, A. M.; Casey, D.; Law, R. V.; Gee, A.; Templer, R. H.; Ces, O. *Chem. Soc. Rev.* **2009**, *38*, 2509−2519.
(81) Seydel, J. K.; Wiese, M. *Drug-Membrane Interactions*; Wiley-VCH Verlag GmbH: Weinheim, 2003.
(82) Maximov, P. Y.; Myers, C. B.; Curpan, R. F.; Lewis-Wambi, J. S.; Jordan, V. C. *J. Med. Chem.* **2010**, *53*, 3273−3283.
(83) Ruenitz, P. C.; Bagley, J. R.; Mokler, C. M. *J. Med. Chem.* **1982**, *25*, 1056−1060.
(84) Wesołowska, O.; Kużdżał, M.; Štrancar, J.; Michalak, K. *Biochim. Biophys. Acta* **2009**, *1788*, 1851−1860.
(85) Van Dael, H.; Ceuterickx, P. *Chem. Phys. Lipids* **1984**, *35*, 171−181.
(86) Boggara, M. B.; Mihailescu, M.; Krishnamoorti, R. *J. Am. Chem. Soc.* **2012**, *134*, 19669−19676.
(87) ACD/Labs. *Advanced Chemistry Development Software* v. 11.2, 1994−2013.
(88) Buchanan, C. M.; Buchanan, N. L.; Edgar, K. J.; Lambert, J. L.; Posey-Dowty, J. D.; Ramsey, M. G.; Wempe, M. F. *J. Pharm. Sci.* **2006**, *95*, 2246−2255.
(89) Faller, B.; Ertl, P. *Adv. Drug Delivery Rev.* **2007**, *59*, 533−545.
(90) Jorgensen, W. L.; Duffy, E. M. *Adv. Drug Delivery Rev.* **2002**, *54*, 355−366.
(91) Lu, W.; Poon, G. K.; Carmichael, P. L.; Cole, R. B. *Anal. Chem.* **1996**, *68*, 668−674.
(92) Bergström, C. A. S.; Wassvik, C. M.; Johansson, K.; Hubatsch, I. *J. Med. Chem.* **2007**, *50*, 5858−5862.
(93) Ahmad, A.; Shahabuddin, S.; Sheikh, S.; Kale, P.; Krishnappa, M.; Rane, R. C.; Ahmad, I. *Clin. Pharmacol. Ther.* **2010**, *88*, 814−817.
(94) Johnson, M. D.; Westley, B. R.; May, F. E. *Br. J. Cancer* **1989**, *59*, 727−738.
(95) Katzir, H.; Yeheskely-Hayon, D.; Regev, R.; Eytan, G. D. *FEBS J.* **2010**, *277*, 1234−1244.
(96) Thomas, P.; Pang, Y.; Filardo, E. J.; Dong, J. *Endocrinology* **2005**, *146*, 624−632.
(97) NIH. http://clinicaltrials.gov/ct2/show/study/NCT01327781 (accessed July 23, 2013).